

Pulse Modulators for Magnetrons

– *Abhijit Tillu*

27.1 Pulsed Magnetron as RF Power Sources for Pulsed Electron Accelerators . . .	262
27.2 Pulse Modulators	262
27.2.1 Line Type Modulator Topology	263
27.3 Case Study: Line Type Magnetron Modulator For Dual Energy Cargo Scanning	267
27.3.1 Magnetron Specifications	269
27.3.2 Capacitor Charging Power Supply	269
27.3.3 Discharging Circuit	269
27.4 Design and Detailed Technical Specification of Individual Sub-system/ Com- ponent	270
27.4.1 Considerations for Pulse Transformer Turns Ratio	270
27.4.2 Pulse Transformer Design	271
27.4.3 Tail Clipper Design	272
27.4.4 De-spiking Network Design	272
27.4.5 Pulse Forming Network	272
27.4.6 Capacitor Charging Power Supply (CCPS)	272
27.4.7 Choice of C_S and L_S	273
27.4.8 Choice of Inverter Transformer Parameters	273
27.4.9 Choice of IGBT Module and Loss Estimation	275
27.4.10 Implementation of Series Resonant Capacitor C_s	276
27.4.11 Implementation of Series Resonant Inductor L_s	276
27.4.12 DC LINK Capacitor	276
27.4.13 Choice of DC Side Inductor	277
27.4.14 Choice of Three Phase Rectifier	277
27.4.15 Heatsink Design	277
27.4.16 Other Subsystems	277
27.5 Concluding Remarks	278

Magnetrons are used as the radiofrequency sources in accelerator cavities. The magnetrons are driven by pulse modulators. In this chapter detailed design of the pulse modulators for magnetron is being provided.

27.1 Pulsed Magnetron as RF Power Sources for Pulsed Electron Accelerators

High Power Pulsed Magnetron are a natural choice for low power Industrial/medical linear accelerators, due to their compactness as compared to klystrons. In simple terms a magnetron is a RF oscillator, which converts input electrical energy into RF signal. The input characteristics of the magnetron are highly nonlinear, and can be best modelled as a biased diode. This is shown in Fig. 27.1. The X axis represents the Cathode to Anode Voltage, and

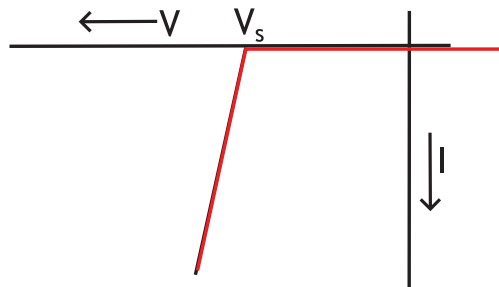


Figure 27.1: V-I Characteristics of Magnetron.

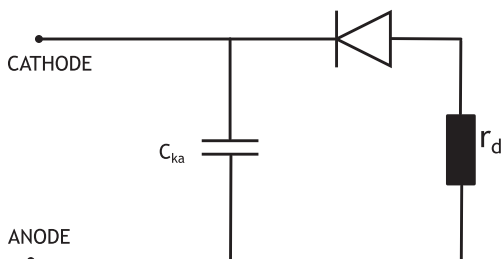


Figure 27.2: Equivalent electrical input model of Magnetron.

the Y axis represents the magnetron current. A typical S-band pulsed magnetron rated for 2 MW peak RF output has V-I operating point of 40 kV/100 A. As indicated in Fig. 27.1, for Magnetron voltage of less than V_s , there is no current flow. However, the current sharply increases after V_s . The static impedance of the magnetron is defined simply as V/I , i.e. 400 Ω , in this example, but the dynamic impedance at the point of operation is $\sim 10\%$ of the static impedance (dynamic impedance, $r_d = dV/dI$).

There is certain capacitance associated with the cathode to anode geometry (C_{ka}), This is typically 50 pF. Hence the Electrical equivalent circuit of a magnetron for all practical cases, is as shown in Fig. 27.2.

To explain the same we refer to the performance characteristics of a typical pulsed magnetron manufactured by e2v technologies (M5028) as seen in Fig. 27.3.

As in Fig. 27.3, the X and Y axes are absolute. As seen in Fig. 27.3, the magnetron's V-I characteristic is function of the applied magnetic field. As the Axial magnetic field is increased from 130 mT to 160 mT, the V-I characteristic curves shift upwards. The Constant RF output and constant efficiency contours are also shown in the same graph. As seen, in order to operate the magnetron at 3 MW peak RF output the operating point has to be -39 kV, 173 A for an axial field of 130 mT or -48.5 kV/127 A for 160 mT field. The Power conversion efficiency is 43-48%.

27.2 Pulse Modulators

Pulse Modulators can be defined as a class of 'POWER CONVERTORS' which converts the AC Mains Power into the required Pulse Power of a well defined pulse shape for driving a

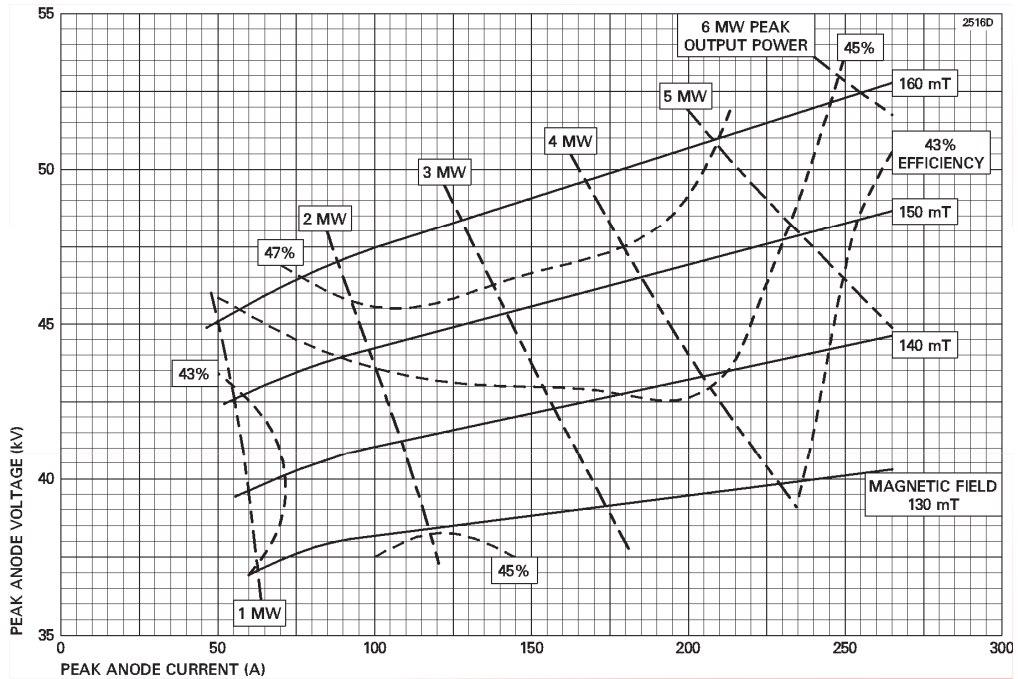


Figure 27.3: Performance chart of M5028.

defined Pulsed Load. As in old school of thought the Pulse Modulators can be classified as shown in the Fig. 27.4. The classification is mainly based on the type of switching, and pulse generation scheme used. In the discussion that will follow, we will discuss only the line type modulator topology in detail.

27.2.1 Line Type Modulator Topology

This is one of the oldest topologies used from the early World War 2 days. The topology is further classified into conventional, command resonant, Capacitor charging, depending on the charging scheme. Fig. 27.5 shows a typical Line type modulator. The circuit operation can be broadly divided as Charging cycle and Discharging cycle. The Discharging cycle, which is central to the process of pulse generation, will be described first.

Before the Discharging cycle the PFN (Pulse Forming Network) capacitors are charged to Twice the applied DC Voltage, as will be explained later. The energy to be transferred to the load in form of pulse is stored as electrostatic energy in the PFN capacitance. The Discharging circuit mainly consists of the PFN, Switch, Pulse transformer and the load.

A. Discharging Circuit

To understand the discharging circuit let us first see the simplified model of the same as shown in Fig. 27.6. The transmission line capacitance is charged to 2 V. Hence the energy stored in the Line is $0.5 C_{line}(2V)^2$ Joules, where C_{line} is the total Capacitance of the open-Circuited Transmission line. A pre-charged transmission line of length (l) can be modelled as a transmission line with no charge, in series with an ideal voltage source of 2 V. The transmission line has a characteristic impedance Z_o , and the velocity of propagation of electromagnetic wave (TEM mode) is v m/s. A detailed mathematical analysis for evaluating

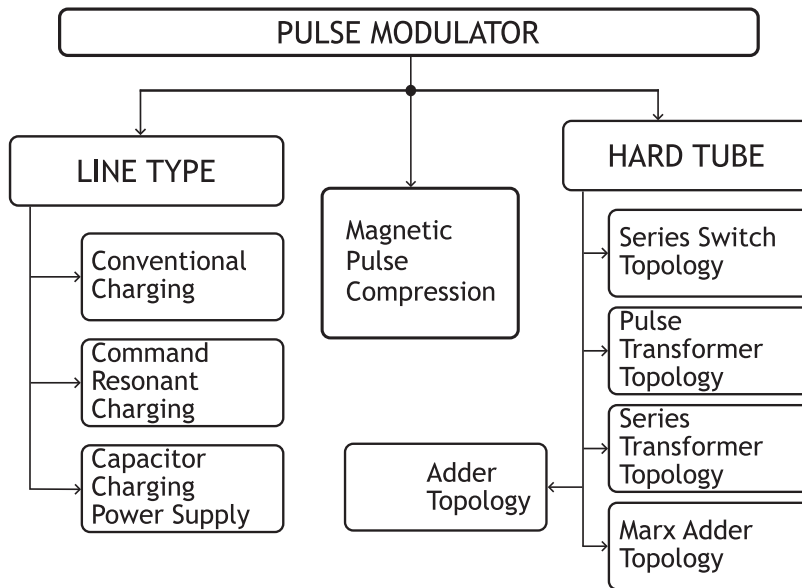


Figure 27.4: A typical classification of pulse modulator topologies.

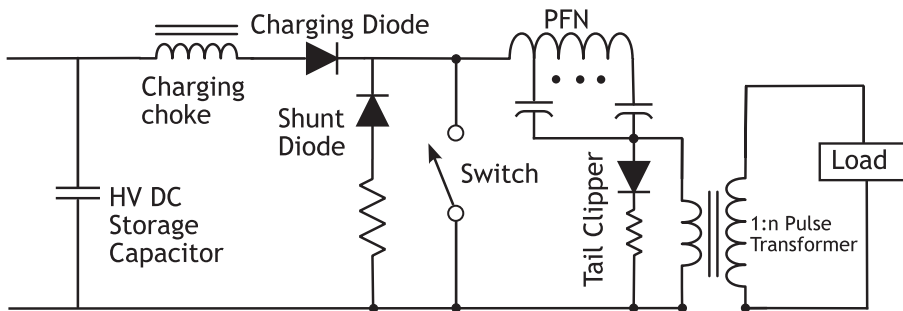


Figure 27.5: A Conventional Line Type Modulator.

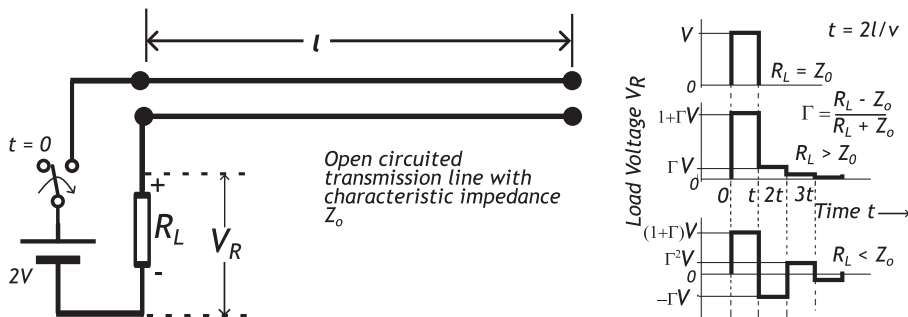


Figure 27.6: A basic line type Discharging Circuit.

the voltage across the load (for various Load Conditions) is covered in tutorial. A simplified explanation for a specific case where $R_L = Z_o$ is as follows. At $t = 0+$, after the switch is

closed, 2 V Volts is divided between the transmission line characteristic impedance Z_o and load resistance R_L .

$$V_R = \frac{2VR_L}{R_L + Z_o} = V, \text{ if } R_L = Z_o \quad (27.1)$$

A voltage wave of magnitude $(2VZ_o)/(R_L + Z_o)$ i.e. V for this special case, propagates along the transmission line with a finite velocity, after the voltage wave has reached the open-circuited end of the transmission line ($z = l$), it is reflected back with the same magnitude and phase. The total time required for the forward wave to propagate from $z = 0$ to $z = l$, is l/v sec, same time will be taken by the reverse moving wave to propagate from $z = l$ to $z = 0$. At $t = 2l/v$, the reflected voltage will add to the forward voltage at $z = 0$, and hence the voltage across the transmission line will be 2 V. The voltage across the load will be simply subtraction of this from 2 V and hence, for the period beyond $t = 2l/v$ and the voltage across the load is zero.

Using the elaborate delay line analysis (see tutorial) for the above problem the voltage across the load can be expressed as

$$V_R(t) = 2V - (1 - \Gamma)u(t) + (1 + \Gamma)(1 - \Gamma)u(t - \frac{2l}{v}) + \Gamma(1 + \Gamma)(1 - \Gamma)u(t - \frac{4l}{v}) + \Gamma^2(1 + \Gamma)(1 - \Gamma)u(t - \frac{6l}{v}) + \Gamma^3(1 + \Gamma)(1 - \Gamma)u(t - \frac{8l}{v}) + \dots \quad (27.2)$$

where, $u(t)$ is a unit step function of time. Here, Γ is the reflection coefficient and is defined as,

$$\Gamma = \frac{R_L - Z_o}{R_L + Z_o} \quad (27.3)$$

As can be seen from Fig. 27.8, $\Gamma = 0$, is the perfect case for maximum energy transfer to the load. The group velocity of the TEM mode in a transmission line (coaxial, strip-line, etc.) is given by

$$v_o = (\mu_o \epsilon_o \epsilon_r)^{-0.5} \text{ m/s} \quad (27.4)$$

Where μ_o is free space magnetic permeability ($4\pi \times 10^{-7}$ H/m), ϵ_o is the free space electric permittivity (8.85×10^{-12} F/m), ϵ_r is the relative permittivity of the dielectric. If we consider a typical solid dielectric transmission line with 50 Ω characteristic impedance, which has a solid dielectric having $\epsilon_r \sim 2.3$, then the velocity of the TEM mode is 66% the velocity of light in vacuum (i.e. 66% of 3×10^8 m/s), then for generating a pulse of 1 μ s the length of the transmission line will be 100 m. For 5 μ s the length will be 0.5 km (Unimaginably long for a High Voltage Transmission line).

Hence instead of using a transmission line for generating such long pulses, the transmission line is approximated by what is called as a Pulse forming network (PFN), where the Distributed capacitance of the transmission line is realized by N number of Bulk Energy Storage Capacitors, and a Bulk Inductance per stage approximates the Distributed Inductance of the transmission line. The Number of stages and the tightness of tolerances in the capacitor parameters, decides how much well the transmission line is approximated by the PFN. If L_{pfn} and C_{pfn} are the total PFN Inductance and total PFN Capacitance respectively, then the characteristic impedance and the Pulse width of the PFN is given by

$$Z_o = \left(\frac{L_{pfn}}{C_{pfn}} \right)^{0.5}, \tau = 2(L_{pfn}C_{pfn})^{0.5} \quad (27.5)$$

There are various types of pulse forming network topologies. Type E and Type D PFN are widely used in klystron modulator applications. Both type E and Type D PFNs have certain

advantages over each other, and this cannot be covered in detail given the vast nature of the topic.

Figure 27.6 shows the ideal case Discharging circuit, where the load is purely resistive and there are no stray elements (inductances and capacitance) that would affect the pulse shape. However such ideal conditions can never exist. As is true in most cases the Load (pulsed klystron), is operated at a very high Voltage (50 kV to 500 kV). Hence HV step up Pulse transformer is used as shown in Fig. 27.5. The PFN impedance, and the pulse transformer ratio are mainly decided by the Forward Blocking Voltage capacity of the Closing Switch (Thyratrons in most of the cases). In some cases, where the RF Source (Klystron/ magnetron) is in a separate Room, far away (few 10s of meters) from the Primary circuit, it becomes desirable to select PFN impedance to be $50/N \Omega$, where N is the number of transmission lines connected in parallel, between the Pulse transformer Primary (in Separate Room), and the Primary Discharge circuit. This is done to ensure that the impedance of the PFN, the transmission line (10s of meters long), and the Load (as seen by the Primary) are all matched. There are a few practical considerations, some of which are mentioned for completeness. They are not elaborated due to the vastness of the topic.

1. A slight negative reflection coefficient is deliberately maintained to ensure thyatron commutation at the end of pulse, in case of conventional resonant charging scheme.
2. The Pulse transformer parameters such as magnetizing inductance result in Droop of the pulse, the Leakage Inductance and Distributed capacitance affect the rise time and overshoot at the start of pulse.
3. The klystron/magnetron electron Gun is basically a diode, hence for any reverse voltage applied across the klystron the impedance is nearly infinite. This results in large back-swing at the end of the pulse (compared to the resistive load case), hence a Resistor Diode combination (called as Tail Clipper) is implemented across the Pulse Transformer Primary, such that it provides a path for reverse current to flow.
4. The HV Electron devices are prone to Arcing, and hence short-circuiting of the load, in that case, there is almost total reflection of Power back to the PFN, and hence resulting in reverse charging of the capacitor, this charge has to be prevented, and removed, Hence a Shunt Diode Resistor combination is connected across the Thyatron. Some designers implement a EOL clipper (End of line Clipper) instead, for taking care of reverse voltage.

B. Charging Circuit

Referring to Fig. 27.5, the PFN charging starts immediately after end of the Pulse when the Switch Commutes. The PFN Inductance is generally within 100 μH , and the charging choke inductance is in 100s of mH to a few H. Hence during the charging cycle the PFN Inductance can be neglected. The charging circuit consists of the Storage capacitance, the Charging Choke (L_c), the Blocking Diode and the total PFN Capacitance (C_{pfn}). The parameters of the charging circuit can be easily calculated by a simple second order ODE. The expression of Charging Voltage and Current are as mentioned below.

$$V_{pfn} = (1 - \cos 2\pi f_0 t) V_{dc}, \quad (27.6)$$

$$I_c = \left[\frac{V_{dc}}{(L_c/C_{pfn})^{0.5}} \right] \sin 2\pi f_0 t \quad (27.7)$$

where $f_0 = [2\pi(L_c C_{pfn})^{0.5}]^{-1}$.

For the above equations to be valid the storage capacitor has to be much larger than the PFN capacitance. As can be seen from the equations, at time, $t = \pi(L_c C_{pfn})^{0.5}$, the current

is at Zero Crossing, and the V_{pfn} is at $2 V_{dc}$. The Blocking Diode D blocks the current from flowing in reverse direction, and hence the PFN retains the voltage of $2 V_{dc}$ unless discharged. This scheme is called Resonant Charging, for reasons, which are obvious to the reader after seeing the above expressions. The Blocking Inductor serves following purposes, namely

1. It isolates the HVDC supply when the Switch is closed. The maximum current drawn from HVDC with Switch S is closed is limited to $V_{dc}t_{on}/L_c$
2. Slowly charges the PFN Capacitors at the required energy

The main disadvantage of this scheme are listed below,

1. The charging cycle starts immediately after the thyratron has commuted. In the event of the thyratron failing to commute, the HVDC is shunted through the blocking inductor.
2. The blocking inductor is designed such that the PFN charges to the desired voltage in time, which is lesser than $1/PRF_{max}$, where PRF_{max} is the maximum pulse repetition frequency. When this pulser is operated at much lower PRF, then the PFN capacitors are unnecessarily stressed at HV for a long time, before discharging.

This conventional line type modulator topology has been the oldest, and the most rugged topology used since the World War II days. The diodes shown in the Fig. 27.5, were vacuum diodes in those period. Eventually with the development of solid-state switches, the charging diodes were replaced by a thyristor series stack. Hence this has an immediate advantage of Command Resonant Charging. The PFN Charging cycle can start sufficiently after the thyratron has commuted. The charging cycle can also be programmed to start just before commencement of discharge cycle, irrespective of how low the operating PRF is. This eliminates both the disadvantages of the earlier conventional scheme. Some designers use one thyratron in the charging circuit, similar to the one used in the discharging circuit. With the development in the IGBT and HF Resonant converter topologies in the last few decades, Constant Current - Capacitor Charging Power Supplies (CCPS) are increasingly becoming more and more popular. As the name suggests, the PFN is linearly charged to the required voltage. The CCPS topology generally uses a HF Series Resonant Converter, the PFN voltage is sensed and the charging cycle is stopped. The complete switching etc is at a Low Voltage (600 V DC Link voltage max), except for output HF transformer secondary & Rectifier. These things make the entire charging circuit much more compact as w.r.t. the earlier mentioned charging schemes, which operate a line frequency and a large chunk of energy is stored in the storage capacitor at High Voltage, as shown in Fig. 27.5. This HF inverter based CCPS has all the advantages of Command Resonant Charging, and it Compact.

Figure 27.7 shows the schematic of a HF Series Resonant Converter Based Charging Circuit. The series resonant converter consisting of L_s , C_s is driven in discontinuous conduction mode. at a constant switching frequency. This ensures Zero Current Switching of the IGBTs. The detailed design considerations of the CCPS are listed in the case study of design of Line type magnetron modulator.

27.3 Case Study: Line Type Magnetron Modulator Design For Dual Energy Cargo Scanning Application

In case of cargo Scanners two distinct electron beam energies are used for material discrimination. To achieve the same the RF pulse power is changed from pulse to pulse.

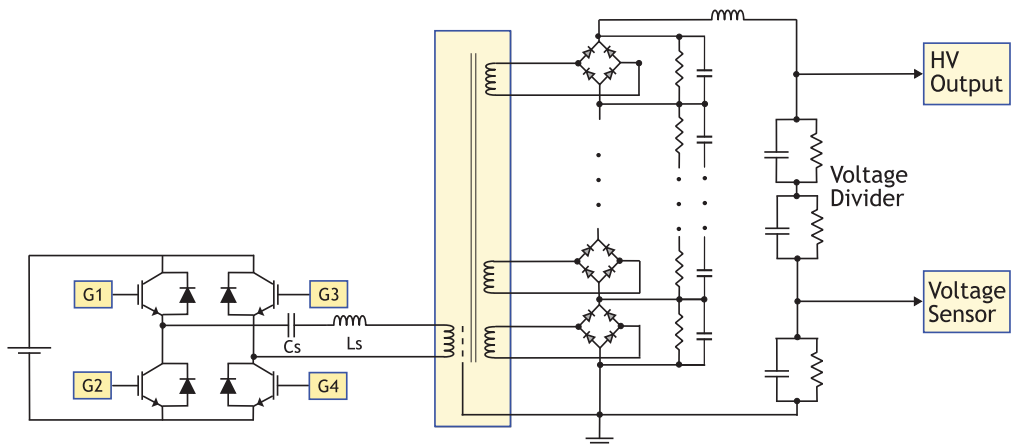


Figure 27.7: HF Series Resonant Converter Based Charging Circuit.

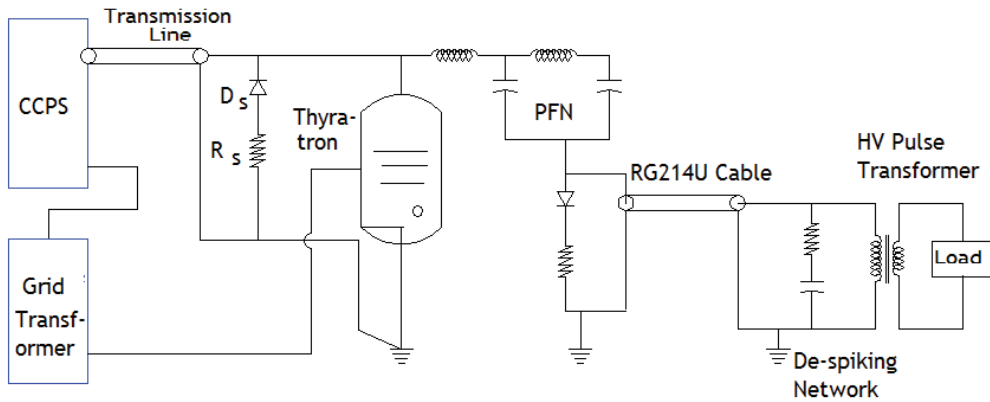


Figure 27.8: Schematic of Line Type Magnetron Modulator.

In this case study we design a magnetron modulator for powering a e2v technologies make M5028 magnetron The magnetron will be operated at 130 mT load-line. (ref Fig 27.9). The typical specifications at the operating point of the magnetron is as mentioned below.

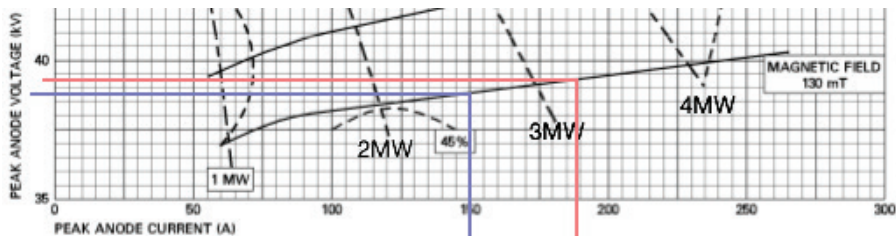


Figure 27.9: Magnetron Load Line.

As indicated in Fig. 27.9, the Red line indicates the typical 6 MeV operating point and the Green line indicates the typical 3 MeV operating point. For detailed data refer to the

datasheet of M5028.

27.3.1 Magnetron Specifications

The operating parameters of Magnetron is tabulated in table 27.1. The topology consists of a

Table 27.1: Operating parameters

Parameter	6 MeV mode	3 MeV mode
Magnetron Peak Power	3.2 MW @ 2856 MHz	2.7 MW @ 2856 MHz
Magnetron Peak Voltage	39.5 kV (-ve)	39.0 kV (-ve)
Magnetron Peak Current	188 A	150 A
Magnetron input pulse width	3.4 μ s	3.4 μ s
Rate of Rise of Pulse Voltage	125 kV/ μ s	125 kV/ μ s
Rise time	300-400 ns	300-400 ns
Pulse repetition freq. (PRF)	250 pps	250 pps

conventional pulse forming network (PFN) based pulse generator. The PFN will be charged by a Constant Current Capacitor Charging Power Supply (CCPS). The PFN will Charge to the set Voltage linearly within \sim 3 ms. On triggering the thyatron, the PFN will dump all its energy into the Load. The Charging and the Discharging Circuits are explained in detail.

27.3.2 Capacitor Charging Power Supply

The Capacitor Charging Power Supply is a IGBT based Constant Current Resonant Converter. It acts as a constant current source for the PFN capacitors. The PFN capacitors are charged to around 20 kV within \sim 3 ms, per charging cycle.

27.3.3 Discharging Circuit

The Discharging Circuit of the modulator is a conventional line type modulator. It basically consists of the PFN, switching thyatron, HV step up pulse transformer with filament heating for load, Tail Clipper, De Spiking network, Shunt Diode, Power transmission line and other Protection and Diagnostic components. The PFN is charged to \sim twice the required primary pulse voltage (in case of matched load). The PFN L and C are chosen such according to the load impedance as seen in the primary and the pulse width requirement. This is discussed in detail later in this report. On receiving a trigger pulse, the thyatron discharges the PFN energy into the load in form of pulse. The Pulse transformer steps up the primary voltage to the desired level, and also ensures proper impedance matching. In most of Cargo Scanning and Medical Linac applications, the Pulse transformer & Load, are in the Linac area, and the modulator is in the Power supply room. Hence Transmission line is used as shown in Fig. 27.1. The Magnetron load, as explained in the earlier can be very well modeled as to have a biased diode type of characteristics. Hence, below a particular negative voltage, it behaves as though it is open circuit. Hence the PFN will see initially a open circuited load. This can lead to voltage spiking; hence a RC series network (Despiking network)is connected across the Pulse transformer Primary. The de-spiking network R_{SNUB} , C_{SNUB} as shown in Fig. 27.1, presents low impedance to the PFN during the rise time. The magnetron will offer a very high impedance to any positive voltage applied to the cathode. Hence this gives rise to high backswing. The Tail Clipper is used to dissipate the energy stored in the magnetizing inductance of the HV pulse transformer and to avoid this excessive back swing. The magnetron Load is prone to intermittent arcing during operation. This can result in PFN

voltage swinging to excessive negative voltages, Hence in-order to limit the negative voltage developed across the thyatron, and to discharge the PFN in this case, shunt diode assembly is connected across the Thyatron. The signal for Arc detection is taken by measuring the current through the shunt diode.

The complete design details are discussed in the following section.

27.4 Design and Detailed Technical Specification of Individual Sub-system/ Component

The modulator is designed for optimum performance in 6 MeV mode, i.e. at 3.2 MW_{pk} RF power.

27.4.1 Considerations for Pulse Transformer Turns Ratio

The pulse transformer with magnetron will be placed in the linac room, and the rest of the modulator in the Power Supply/Control Room. The cable length in-between will be typically approximately 20 m (if not more). In such case, it is strongly recommended that the load impedance as seen by the transmission line be equal to the characteristic impedance of the transmission line. Commercially available HV coaxial transmission lines (RG214U) have a characteristic impedance of 50 Ω. N such coaxial cables can be connected in parallel to have a effective characteristic impedance of 50/N Ω. Hence the first binding condition for deciding the turns ratio of HV pulse transformer is that the load impedance as seen by the primary, will be 50/N Ω. This being satisfied, the availability of thyatron and other components also influences in the optimum choice of turns ratio. For a 1:n pulse transformer, the impedance as seen by the primary is given as $Z_{load}/(n^2)$. Table 27.2 summarizes the effect of using N no. of RG214U in parallel (N = 1 to 4). It states that the primary Voltage (V_{pri}), and hence Thyatron Voltage (V_{thy} = twice V_{pri}), primary Current (I_{pri}).

The modulator is designed for optimum performance at 3.2 MW RF power. Referring to the load line indicated in Fig. 27.2, and the parameters given in Table 27.3, the static impedance of the magnetron at 3.2 MW is 210 Ω (39.5 kV/188 A). The energy per pulse considering a pulsewidth of 3.8 μs is 28.2 J.

Table 27.2: Modulator parameters as a function of choice of characteristic impedance.

Number of cables, N	1	2	3	4	5
Effective primary impedance (Ω)	50	25	16.66	12.5	10
Step up ratio, n	2.05	2.9	3.55	4.1	4.58
V_{pri} (kV)	19.27	13.62	11.13	9.63	8.62
V_{thy} (kV)	38.55	27.24	28.26	19.26	28.24
I_{thy} (peak) (A)	385.4	545.2	667.4	770.8	861.04
I_{thy} (avg) (A)	0.37	0.52	0.63	0.73	0.82
I_{thy} rms (A)	11.9	16.9	20.7	23.9	26.7
I_{rms} per coaxial	11.9	8.5	6.9	6	6.7
C_{pfn} total (nF)	38	76	114	152	189
In these calculations it is assumed that, the pulse width is 3.8 μs.					

From **Table 27.2** it is evident that if only one 50 Ω cable is used, then the thyatron has to be operated at 38.55 kV, and if 5 cables are used the thyatron operating point is 17.24 kV. In any case the peak and average currents are less than 1 kA and 1 A respectively. Reliable

Glass thyratrons from e2v technologies are available for peak currents of 1 kA and average current of 1.25 A. The thyratrons are naturally cooled, and are comparatively cheaper as compared to their ceramic counterparts. From Table 27.2, it is also clear that if Number of Cables are chosen as 3 or 4, then CX1140 thyatron can be utilized, most efficiently. As we are reducing the characteristic impedance further, the average current is approaching the maximum current rating of the thyatron (CX1140). Characteristic Impedance of 12.5Ω was chosen over 16.66Ω , so as to reduce the voltage requirement on the CCPS.

Summarizing the Above Discussion

Step up ratio of HV Pulse transformer	: 4.1
PFN Impedance	: 12.5Ω
Number of Coaxial Transmission lines	: 4, RG214/U connected in parallel
Pulse Width Flat Top	: $3.8 \mu s$
Thyatron	: CX1140, Make, e2V

27.4.2 Pulse Transformer Design

The specifications are again summarized in Table 27.3 for Input Parameter of Pulse Transformer Design. Hitachi metglas make Powerlite cores based on Iron based metglas alloy

Table 27.3: Pulse transformer Design Specifications.

Step up ratio	4.1
Primary Peak Voltage (kV)	9.63
Primary Peak Current (A)	770
Primary Pulse width (μs)	3.8
Max Pulse Repetition Freq. (pps)	250
Primary RMS Current (A)	24
Secondary Peak Voltage (kV)	39.5
Secondary Peak Current (A)	188
Rse Time of secondary Voltage (ns)	500
Total Secondary RMS Current (A)	6
In calculation of primary rms current, the contribution of magnetizing current is neglected.	

2605SA1 are suitable for this application. These Amorphous Cut C cores are made of ribbon of $25 \mu m$ (~ 1 mil) of amorphous material. These low loss cores are used generally in transformer and inductor applications for High freq. inverters, choppers etc. The largest core, locally available is AMCC 1000.

The 1:4.1 HV pulse transformer will use two numbers of AMCC1000 pairs. The winding will be bifilar type (secondary) with provision for providing Filament power to the magnetron. The number of turns in the primary is 10.T. The primary winding will be accomplished by using a 6 mm wide and ~ 1 mm thick Copper Strip.1-2 mm spacing will be allowed between turns. The total winding length of ~ 70 mm will be maintained. The secondary will consist of 41 turns SWG 16 (Wire Diameter is 1.626 mm), There is no need for Core Biasing/Reseting, as the Br for these cores is 250 mT. The transformer will be oil insulated.

27.4.3 Tail Clipper Design

From the pulse transformer design, it is estimated that the magnetizing inductance as seen in the primary is ~ 2.5 mH (min). The magnetizing current will be ~ 15 A, and the energy stored in the magnetizing inductance is ~ 0.3 J. This energy is dissipated in the Tail Clipper Resistor. Hence the Total Power Dissipated in the Tail Clipper, at PRF of 250 pps will be 0.3 J times $250 = 75$ W. In the magnetron datasheet it is recommended that the backswing should not exceed 10% of the pulse voltage. If the backswing is limited to 5%, i.e. ~ 2 kV across the magnetron, then the backswing in the primary will be ~ 500 V. Hence the Tail Clipper Resistance will be $500/15 = 33 \Omega$. Hence the Tail Clipper Resistor will be Wire Wound (Preferably Non-Inductive) $30 \Omega / 500$ W. 10 times L_m/R is ~ 1 ms, whereas the min period between consecutive pulses is 4 ms. Hence there is no fear of any Volt Second Instability in the Pulse Transformer, and hence the transformer slowly going into saturation. The tail Clipper is implemented using a series combination of wire wound resistors and fast recovery Diodes (SF 5408).

27.4.4 De-spiking Network Design

The RC De-spiking network is connected across the pulse transformer primary. Magnetron acts like a Bias Diode load, hence the impedance of the magnetron is very high below a particular knee voltage. This can give rise to spiking during the rise time. The RC time constant is adjusted such that the PFN sees impedance close to the characteristic impedance during the Rise time. R is 12.5Ω , C will be 5 nF or 10 nF. The rate of rise will be the deciding factor for choice of the capacitor. This has to be experimentally chosen. The Energy loss to the De-spiking network is given by $C(V^2)$, C is 10 nF and V is ~ 10 kV. The loss per pulse is 1 J. Hence, at 250 Hz, the Power loss is 250 W. The despiking network has to be placed in the closed vicinity of the pulse transformer, i.e. on the other side of the transmission line.

27.4.5 Pulse Forming Network

The estimated value of PFN capacitance is 150 nF (see table 27.2), 8 number of 20 nF / 30 kV will be used for the application. For a characteristic impedance of 12.5Ω , the total PFN inductance is 25 H, The PFN inductor will be constructed using a $1/8$ inch copper tube. The rms current in the PFN coil is 24 .

Hence, the PFN Specifications are summarized:

PFN Impedance	: 12.5Ω
Pulse Width Flat Top	: $3.8 \mu s$
Total PFN Capacitance	: 160 nF
Total PFN Inductance	: $25 \mu H$
Number of Stages	: 8
Capacitor per stage	: 20 nF/ 40 kV
ESL of capacitor	: < 50 nH
Peak Current Handling Capacity	: 2 kA
Rms Current/ capacitor	: < 4 A

Guillemin E type PFN may be preferred to the D type.

27.4.6 Capacitor Charging Power Supply (CCPS)

From Table 27.2 it is clear that the PFN will be charged to 19.3 kV maximum. The minimum period between two pulses is 4 ms. Typically 0.2 ms dead time is allowed for the thyatron to recover after the discharging cycle. Hence it will be safe to design CCPS with a charging time of 3.3 ms. Fig. 27.10 shows the typical PFN charging waveform.

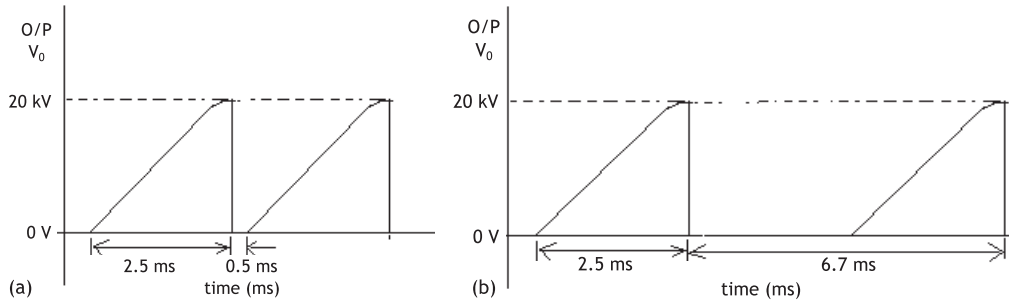


Figure 27.10: (a) CCPS Output @ ~300 pps, and (b) CCPS output at 150 pps.

Table 27.4: CCPS Input Parameters for Design.

Sl. No.	Parameter	Value
1	Output Energy per pulse in 3.2 MW mode (J)	28.2
2	Pulse Repetition Frequency, $1/T_{PRF}$ (pps)	250
3	CCPS Efficiency (%)	90
4	Charging Rate, P_c (kJ/s) = $28.2\text{J} / 0.9 / 3.3$ ms	9.5
5	RMS Input Voltage to CCPS, 3-phase Line - Line (V)	$415 \pm 10\%$
6	Worst Case DC Link Voltage, V_{DCLINK} , min (V)	500
7	Typical CCPS Output Voltage V_o , typ (kV)	19.5
8	PFN Capacitance, C_{pfn} (nF)	160

Table 27.4 summarizes the input parameters for the design of CCPS. The choice of various components/ subsystems will be so as the satisfy the above mentioned Design Parameters.

27.4.7 Choice of C_S and L_S

$$P_c = (0.5)(2V_{DCLINK})^2 C_S k f_s \quad (27.8)$$

Where,

P_c : Charging rate

V_{DCLINK} : DC Link Voltage

C_S : Series Resonant Capacitor

f_s = Total switching frequency (twice the individual IGBT Switching Frequency)

$k = 0.8$ at $V_{DCLINK} = 500$ V, CCPS Output Voltage = 19.5 kV.

Hence, C_S and f_s are estimated as 330 nF and 72 kHz respectively. Allowing a Dead Band of $\sim 2 \mu\text{s}$, the Resonant Frequency (f_o) is chosen as 83.34 kHz. Hence, Resonant Inductance $L_S = 11 \mu\text{H}$. The Characteristic Impedance $Z_o = 5.77 \Omega$.

27.4.8 Choice of Inverter Transformer Parameters

Inverter transformer turns ratio:

For $k = 0.8$ at $V_{DCLINK} = 500$ V; CCPS Output Voltage = 19.5 kV; the effective reflected voltage in the primary is $500 \times 0.8 = 400$ V. Hence, the desired turns ratio is $19.5 \text{ kV} / 400 = 48.75$. The core selected is a ferrite Toroidal core of OD 140 mm, ID 106 mm, HT 25 mm

(magetic Inc make OP; Two such cores will be used). Hence the effective core cross-section is 2×422 sq. mm. The min number of turns in the secondary (N_s) is given by Eq. (27.9),

$$N_s = \frac{V_o}{2f_s A_c B_{max}} \quad (27.9)$$

where,

V_o = output Voltage, 19.5 kV

f_s = 72 kHz

A_c = 2×422 sq. mm

B_{max} = 0.28 T

Hence, N_s = 573 Turns minimum.

Since, the Inverter Transformer is implemented using 38 independent centre-tap windings the best fit is $N_p = 12$ turns and $N_s = 16 \times 38 = 608$ turns. The effective turns ratio (n) is $608/12 = 50.66$. This is slightly more than the desired turns ratio of 48.75. However, this does not affect the design significantly, as there is only 4% reduction in K, and hence this will imply a charging time of ~ 3.43 ms, instead of 3.3 ms. This is acceptable. Under worst cases scenario, the switching frequency can be increased to 74.8 kHz, keeping all other parameters constant. All the calculations that will follow will use turns ratio (n) as 50.66 and $f_s = 72$ kHz.

Table 27.5: CCPS Resonant Circuit Components.

Sl. No.	Parameter	Value
1	Series Resonant Capacitance, C_S (nF)	330
2	Series Resonant Inductance, L_S (μ H)	11
3	Resonant Frequency, f_o (kHz)	83
4	Switching Frequency, f_s (kHz)	72
5	Characteristic Impedance, Z_o (Ω)	5.77
6	Inverter Transformer Turns Ratio, n	50.66

The estimated rms current in the primary resonant circuit ($I_{rms,pri}$) is estimated as follows:

$$I_o = \frac{V_{DCLINK}}{Z_o} \quad (27.10)$$

$$I_{rms,pri} = I_o \sqrt{0.5 \frac{T_c}{T_{PRF}} \frac{f_s}{f_o} (1 + 0.33k^2)} \quad (27.11)$$

Average charging current ($I_{avg,sec}$) is given by:

$$I_{avg,sec} = \frac{I_o}{n} (2/) \frac{f_s}{f_o} \quad (27.12)$$

Accordingly, the charging time (T_c) is given as Eq. (27.13).

$$T_c = C_p f n \frac{V_o}{I_{avgsec}} \quad (27.13)$$

The peak and average IGBT Current is given Eqs. (27.14) and (27.15).

$$I_{IGBT,pk} = (1 + k)I_o \quad (27.14)$$

$$I_{IGBT,avg} = (2 + k)I_o \frac{T_c}{T_{PRF}} \frac{f_s}{f_o} \frac{0.25}{3.14} \quad (27.15)$$

The peak antiparallel diode current (in Full Bridge Inverter) is same as I_o , the average current in the antiparallel diode is given by Eq. (27.16).

$$I_{DIODE,avg} = (2 - k)I_o \frac{T_c}{T_{PRF}} \frac{f_s}{f_o} \frac{0.25}{3.14} \quad (27.16)$$

Table 27.6: Circuit Currents at two extreme DC Link Voltages

V_{DCLINK} (V)	I_o (A)	$I_{avg,sec}$ (A)	T_c (ms)	k	$I_{rms,pri}$ (A)	$I_{IGBT,pk}$ (A)	$I_{IGBT,avg}$ (A)	$I_{DIODE,avg}$ (A)
500	86.7	0.94	3.32	0.77	56.8	153.5	13.7	6.1
600	104	1.12	2.76	0.64	60.2	170.6	13	6.7

27.4.9 Choice of IGBT Module and Loss Estimation

Based on the parameters listed in Table 27.6, the infineon make Dual Fast IGBT module FF150R12KS4 has been chosen. Two such modules will be used to form a Full Bridge. IGBT Loss estimation (per IGBT):

Conduction Loss:

As indicated in Table 27.6, avg IGBT current is 13.7 A max. IGBT data-sheet suggests, $V_{ce,sat}$ of 3.85V, typ. at 150 A;

Hence the conduction Loss per IGBT is $(13.7 \times 3.85) = 53$ W.

Switching Loss per IGBT is combination of two losses, viz. turn ON Loss and Turn OFF Loss. The turn Off loss in this case is negligible by virtue of the topology. During Turn On, there are two loss mechanisms considered, namely the loss during the rise time, and the loss associated with the discharge of IGBT output capacitance in the IGBT. For a worst case estimate of the loss associated with the finite rise time, it is assumed that the Vce is not changing and is held at 600V during the current rise time. The current is increasing sinusoidally towards $I_{IGBT,pk}$. The IGBT data-sheet indicates a typical rise time (t_r) of 70 ns. A rise time of 100 ns is considered for loss estimation.

$$P_{loss,1} = V_{DCLINK} I_{IGBT,pk} \frac{f_s \cos(2\pi f_o t_r) - 1}{2 \cdot 2\pi f_o} \quad (27.17)$$

It should be noted that the $I_{IGBT,pk}$ is increasing linearly from I_o to $(1 + k) I_o$, over the time T_c . A worst case $I_{IGBT,pk} = 170$ A, $V_{DCLINK} = 600$ V is considered for estimation.

$$P_{I,IGBT,pk} = 9.6 \text{ W} \quad (27.18)$$

$$P_{loss,2} = \frac{f_s}{2} \frac{1}{2} \frac{4C_{oess}}{3} (V_{DCLINK})^2 \quad (27.19)$$

Data of C_{oess} not available. Based on the data available from equivalent IGBT (Semokron) C_{oess} is estimated to be 2 nF.

$$P_{loss2} = 17.1 \text{ W} \quad (27.20)$$

Hence the total switching loss per IGBT is estimated to be

$$P_{loss} = P_{loss,1} + P_{loss,2} = 26.7 \text{ W} \quad (27.21)$$

Total loss per IGBT is sum of switching and conduction loss

$$P_{loss,perIGBT} = 79.7 \text{ W} \quad (27.22)$$

The typ. Forward voltage for the antiparallel diode is 2 V, hence the diode conduction loss is estimated to be

$$P_{loss,DIODE} = V_F I_{DIODE,avg} = 2 \times 6.7 = 13.4 \text{ W} \quad (27.23)$$

The diode storage charge and hence Err is extremely small as dI_F/dt is very slow, and hence neglected.

Hence the total loss per IGBT/Diode Combination is $79.7 + 13.4 = 93.1 \text{ W}$;

Hence the total loss for two Dual modules is $93.1 \times 4 = 373 \text{ W}$.

27.4.10 Implementation of Series Resonant Capacitor C_s

The series resonant capacitance of 330 nF is implemented using conduction cooled capacitors. Alcon male FP-4-150 SP 330 nF/ 700 V_{rms} capacitors will be used. 42 such capacitors will be connected in parallel to form a pair. Two such pairs will be connected in series to implement a 330 nF/ 1400 V_{rms} Capacitor assembly.

27.4.11 Implementation of Series Resonant Inductor L_s

The Series resonant inductor will be implemented with two ferrite cores (2 pairs of UU100). It is estimated that the leakage inductance of the Inverter Transformer is $\sim 5 \mu\text{H}$, as seen from the primary. Hence a series inductance of 6 μH has to be implemented.

$$LI_{pk} = N A_c B_{max} \quad (27.24)$$

where, $L \sim 6 \mu\text{H}$

$I_{pk} = I_{IGBT,pk} = 170 \text{ A}$

$B_{max} = 0.2 \text{ T}$

$A_c = 2 \times 620 \text{ sq. mm}$

Hence $N = 4$ turns

Air gap

$$l_g = \frac{\mu_o A_c N^2}{L} \quad (27.25)$$

Hence $l_g \sim 4 \text{ mm}$, i.e. 2 mm each side

In order to make the inductance more predicable, and reduce the stray fields, the winding length should be as long as possible. Hence the entire winding length of 100 mm should be occupied. Both the arms of the winding will be used, Each arm contains 4 turns. These arms will be driven in parallel. One arm is wound counterclockwise, and the other is wound clockwise. The winding has to be implemented with litz wire of $\sim 10 \text{ sq mm}$ at least, so as to restrict the current density to 3 A/sq mm.

27.4.12 DC LINK Capacitor

The energy transferred per pulse from the C_{DCLINK} to the PFN is $\sim 31 \text{ J}$. Hence the energy stored in C_{DCLINK} should be at-least 310 J ($10 \times 31 \text{ J}$). The minimum V_{DCLINK} is 500 V, hence,

$$\frac{1}{2} (C_{DCLINK}) (V_{DCLINK})^2 > 310 \text{ J} \quad (27.26)$$

Hence C_{DCLINK} should be at-least 2.48 mF. As indicated the rms current in the primary circuit is 60 A. C_{DCLINK} is implemented using metalized polypropylene Capacitors Alcon electronics make Aluminum body metalized polypropylene capacitors (DCL 41) can be used for this implementation. Only 3 nos. of 1080 $\mu\text{F}/700\text{ V}$ are necessary in this case Each capacitor is of Dia 116 mm and Ht. 140 mm.

27.4.13 Choice of DC Side Inductor

The DC side inductor has been chosen to be 10 mH. The choice is based on simulations results.

27.4.14 Choice of Three Phase Rectifier

The maximum average current in the rectifier output is 16 A. Hence Semikron make Power Bridge Rectifier module SKD31/12, rated for 44 A/ 1200 V ($T_c = 85^\circ\text{C}$) or IXYS make VUO30-12NO3 is suitable, for the application.

Power Dissipation in the Rectifier module is estimated to be 39 W $\{(16\text{ A} \times (2 \times 1.2\text{ V}))\}$.

27.4.15 Heatsink Design

The two IGBT modules and the rectifier Diode assembly will be housed on the same heatsink. Hence the total Heat load on the Heatsink is 412 W (373 + 39). An Appropriate Extruded Aluminium heatsink with Forced air cooling with 0.08 k/W thermal resistance is sufficient. For a worst case ambient temperature of 55°C (In the vicinity of heatsink), the IGBT junction temperature will be $< 90^\circ\text{C}$. There are many Extruded heatsink manufacturers in India, Unfortunately, detailed data is not available from the indian manufacturers w.r.t. the thermal resistance (as a function of airflow) of these heatsinks. Hence for a heat load of 412 W, the maximum rise in case temperature is expected to to 33°C .

For a worst case ambient of 55°C , the estimated heat sink temperature is 88°C .

The thermal resistance for the module FF150R12KS4 for IGBT is $0.1 + 0.03 = 0.13\text{ k/W}$.

Hence the estimated junction temperature for the IGBT is $[88 + (79.7 \times 0.13)] = 99^\circ\text{C}$.

The thermal resistance for the module FF150R12KS4 for Diode is $0.25 + 0.06 = 0.31\text{ k/W}$.

Hence the estimated junction temperature for the IGBT is $[88 + (13.4 \times 0.31)] = 92^\circ\text{C}$.

The devices in the IGBT module (FF150R12KS4) are rated to operate at junction temperature of 125°C . Hence the choice of the device and the heatsink is optimum.

The thermal resistance (junction to heat sink) in case of IXYS make VUO30-12NO3 is 2.4 k/W per diode. Hence the Modules thermal resistance from junction to heat sink is $2.4/6 = 0.4\text{ k/W}$. Hence the junction temperature is expected to be $[88 + (39 \times 0.4)] = 104^\circ\text{C}$. The device is rated for a maximum junction temperature of 150°C . In case of Semikron make, the modules thermal resistance from junction to heat sink SKD31/12 is 0.43k/W. Hence the junction temperature is expected to be $[88 + (39 \times 0.43)] = 105^\circ\text{C}$. The device is rated for a junction temperature of 125°C . In ether case the choice is optimum.

27.4.16 Other Subsystems

The other subsystems such as the thyatron grid trigger circuit, Thyatron voltage sensing and interlock generator and soft start for filament heating of the thyatron, will be discussed in brief, below. The trigger generator generates a 1 kV pulse of pulse width $\sim 2\mu\text{s}$ across the thyatron Grid to cathode (unloaded).

The thyatron and magnetron have a heating time of 5 minutes minimum. It is recommended to have a soft start for the thyatron, so as to ensure long filament life.

Magnetron filament heating power supply and Programmable heating

Prior to application of anode voltage, the magnetron heater voltage should be 13 V for at least 6 min. Within 30 sec, after application of anode voltage the heater voltage should be reduced to as a function of mean input power as mentioned in the thyratron data sheet (page 3). The voltage is reduced to 6 V at 6 kW to 7 kW average input power to the magnetron. Refer to detailed magnetron Data sheet for detail Magnetron Electromagnet Power Supply. The electromagnet is required to provide 130 mT. The electromagnet has a power consumption of 1.5 kW at 165 mT, and it will be ~ 1.2 kW at 28 A, corresponding to 130 mT. Hence a 50 V/ 40 A (2 kVA), constant current power supply is required for powering the electromagnet.

27.5 Concluding Remarks

The reader has been introduced to the detailed design philosophy used for implementation of a line type modulator for magnetron. The detailed design of Inverter Transformer, HV Pulse transformer has been skipped in this introduction. The design covers detailed consideration specific of Pulse High Power magnetron load with a case study.

Suggestions for Further Reading

- a) [139–143]

Tutorial

1. Derive the expression for charging rate, in case of series resonant converter operated in discontinuous conduction mode, at constant switching frequency.

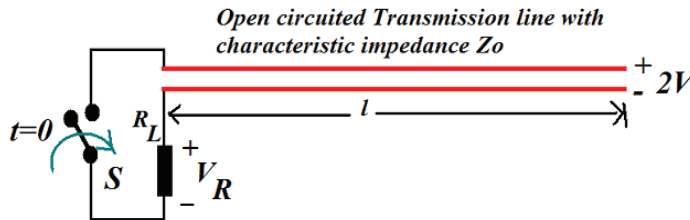


Figure 27.11: Open circuit transfer line for charging rate problem.

Solution

In order to find the expression for the charging rate, let us refer the PFN Capacitor and the charging voltage to the primary of the inverter transformer. The PFN Capacitor C_{pfn} is linearly charged at a constant current I_{avg} from ZERO to the Set voltage V_o . The energy per pulse is given by

$$U = \frac{1}{2} C_{pfn} V_o^2 \quad (27.27)$$

Hence the Charging rate is given by

$$P_c = \frac{U}{T_c} \quad (27.28)$$

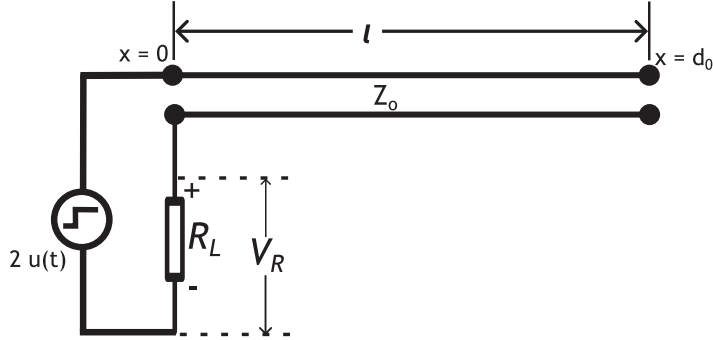


Figure 27.12: Equivalent circuit of above transfer line for charging rate problem.

$$V_o = \frac{I_{avg} T_c}{C_{pfn}} \quad (27.29)$$

as the capacitor is charging linearly.

$$C_{pfn} = \frac{I_{avg} T_c}{V_o} \quad (27.30)$$

Hence we replace for C_{pfn} from Eq. (27.30) in Eq. (27.27).

$$U = \frac{1}{2} (I_{avg} T_c V_o) \quad (27.31)$$

Replacing for U from Eq. (27.31) in Eq. (27.28)

$$P_c = \frac{1}{2} (I_{avg} V_o) \quad (27.32)$$

In case of series resonant converter operating in Discontinuous conduction mode the following is the resonant current given by

$$I_o = \frac{V_{DC}}{Z_o} \quad (27.33)$$

Where, is the characteristic impedance given by

$$Z_o = \left(\frac{L_s}{C_s} \right)^{0.5} \quad (27.34)$$

$$I_{avg} = I_o \left(\frac{2}{\pi} \right) \frac{T_o}{T_s} \quad (27.35)$$

T_s is the switching period, $T_s - T_o$ is the dead time in between two resonance cycles Resonance period is given by

$$T_o = 2\pi \left(\frac{L_s}{C_s} \right)^{0.5} \quad (27.36)$$

Substituting for I_o and T_o in Eq. (27.36), from Eq. (27.33) and Eq. (27.36)

$$I_{avg} = \frac{V_{DC}}{Z_o} 4 \left(\frac{Ls}{C_s} \right)^{0.5} \frac{1}{T_s} \quad (27.37)$$

Substituting for Z_o from Eq. (27.34) in Eq. (27.37)

$$I_{avg} = \frac{V_{DC} 4 C_s}{T_s} \quad (27.38)$$

Substituting for I_{avg} from Eq. (27.39) in Eq. (27.32)

$$P_c = \frac{1}{2} \frac{4 V_{DC} V_o C_s}{T_s} \quad (27.39)$$

But

$$V_o = k V_{DC} \quad (27.40)$$

$$f_s = 1/T_s \quad (27.41)$$

Hence proved,

$$P_c = \frac{1}{2} (2 V_{DC})^2 k C_s f_s \quad (27.42)$$

2. Derive the expression for the output of line type pulser implemented as shown in the Fig. below:

The Pulse forming line (PFL) of length l meters and characteristic impedance Z_o Ω is charged to 2 V. The switch is closed at $t = 0$.

Solution

The circuit shown above can be represented mathematically as follows:

Equivalent Mathematical representation The Precharged PFL (like a capacitor) can be represented as a PFL with Zero charge in series with an ideal voltage source.

At $t = 0$ the disturbance is launched into the PFL. The source sees the PFL impedance (Z_o) in series with the Load R_L . Hence the voltage wave launched into the PFL is given by

$$V_{11}(t) = \frac{2u(t)Z_o}{Z_o + R_L} = (1 - \Gamma)u(t) \quad (27.43)$$

where

$$\Gamma = \frac{R_L - Z_o}{(Z_o + R_L)} \quad (27.44)$$

is defined as the reflection coefficient.

The above expression is the magnitude of voltage across the PFL at $x = 0$. This wave propagates with a velocity v_o m/s toward $x = d$, and sees a discontinuity (open circuit) at $t = l/v$ sec. The wave is reflected without any change in the magnitude or the phase at $x = d$. Mathematically the reflected wave can be considered to be launched from a voltage source at $x = d$. This is shown in the equivalent circuit below:

This voltage wave, $(1 - \Gamma)u(t - l/v_o)$ propagates towards $x=0$ and after propagating for l/v_o sec, sees a discontinuity at $x = 0$. Hence the voltage developed at $x=0$, is given by

$$V_{12} = (1 - \Gamma)(1 + \Gamma)u \left(t - \frac{2l}{v_o} \right) \quad (27.45)$$

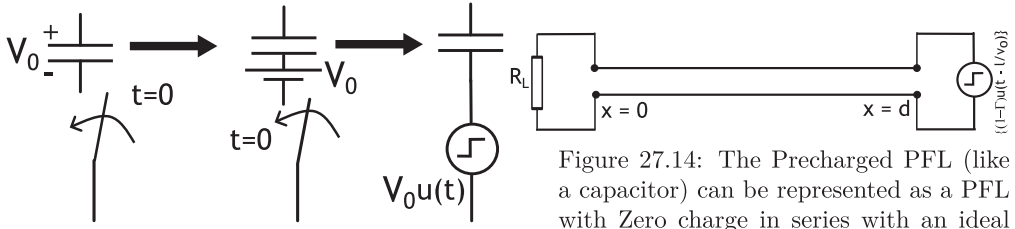


Figure 27.13: Equivalent Mathematical representation.

Figure 27.14: The Precharged PFL (like a capacitor) can be represented as a PFL with Zero charge in series with an ideal voltage source..

The magnitude of voltage wave reflected back towards $x = d$ is given as

$$V_{r1} = (1 - \Gamma)\Gamma u\left(t - \frac{2l}{v_o}\right) \quad (27.46)$$

V_{r1} will be modeled as a fresh voltage source of magnitude $\Gamma(1 - \Gamma)$ at $x = 0$ & at $t = 2l/v_o$. Following the above treatment we understand that this wave reflects at $t = 3l/v_o$, and arrives at $x=0$ again at $t = 4l/v_o$. Hence the magnitude of the voltage developed by this wave at $x = 0$ is given as

$$V_{l3} = \Gamma(1 - \Gamma)(1 + \Gamma)u(t - 4l/v_o) \quad (27.47)$$

The magnitude of voltage wave reflected back towards $x = d$ is given as

$$V_{r2} = \Gamma(1 - \Gamma)\Gamma u(t - 4l/v_o) = (1 - \Gamma)\Gamma^2 u(t - 4l/v_o) \quad (27.48)$$

Continuing the above treatment we have

$$V_{l4} = \Gamma^2(1 - \Gamma)(1 + \Gamma)u(t - 6l/v_o) \quad (27.49)$$

$$V_{l5} = \Gamma^3(1 - \Gamma)(1 + \Gamma)u(t - 8l/v_o) \quad (27.50)$$

And So on... Hence the voltage across the PFL at $x = 0$ is given by superposition of all the voltages $V_{l1}, V_{l2}, V_{l3}, V_{l4}, V_{l5} \dots$

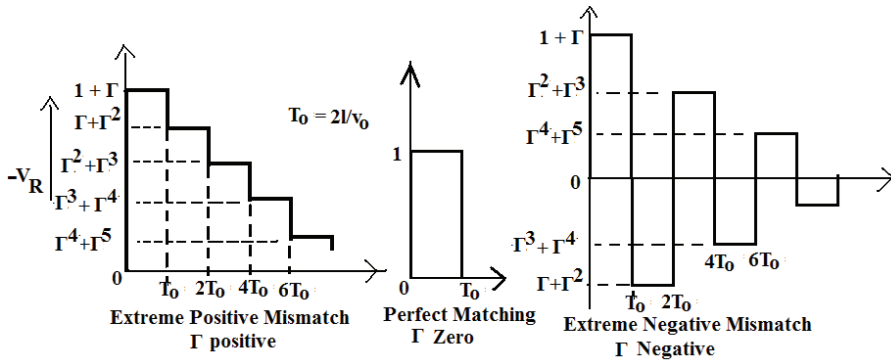


Figure 27.15: The representation of three cases: Extreme positive mismatch (left), perfect match (middle) and extreme negative mismatch (right).

$$V_l(t) = (1 - \Gamma)u(t) + (1 + \Gamma)u\left(t - \frac{2l}{v_o}\right) + \Gamma(1 + \Gamma)u\left(t - \frac{4l}{v_o}\right) + \Gamma^2(1 + \Gamma)u\left(t - \frac{6l}{v_o}\right) \dots \quad (27.51)$$

Hence, the voltage across the load resistance will be:

$$V_R(t) = V_l(t) - 0.2 - V_R(t) = 2 - (1 - \Gamma)u(t) + (1 + \Gamma)u\left(t - \frac{2l}{v_o}\right) + \Gamma(1 + \Gamma) \quad (27.52)$$

$$u\left(t - \frac{4l}{v_o}\right) + \Gamma^2(1 + \Gamma)u\left(t - \frac{6l}{v_o}\right) \dots$$

Note: The above mathematical treatment is applicable only in case of a purely resistive load, whose resistance is independent of applied voltage. This however is not the case in case of klystrons/ magnetrons.